

## Effect of a highly concentrated lipopeptide extract of *Bacillus subtilis* on fungal and bacterial cells

Augusto Etcheagaray · Carolina de Castro Bueno · Itamar Soares de Melo ·  
Siu Mui Tsai · Marli de Fátima Fiore · Maria Estela Silva-Stenico ·  
Luiz Alberto Beraldo de Moraes · Omar Teschke

Received: 29 January 2008 / Revised: 30 June 2008 / Accepted: 3 July 2008 / Published online: 25 July 2008  
© Springer-Verlag 2008

**Abstract** Lipopeptides produced by *Bacillus subtilis* are known for their high antifungal activity. The aim of this paper is to show that at high concentration they can damage the surface ultra-structure of bacterial cells. A lipopeptide extract containing iturin and surfactin ( $5 \text{ mg mL}^{-1}$ ) was prepared after isolation from *B. subtilis* (strain OG) by solid phase extraction. Analysis by atomic force microscope (AFM) showed that upon evaporation, lipopeptides form large aggregates ( $0.1\text{--}0.2 \mu\text{m}^2$ ) on the substrates silicon and mica. When the same solution is incubated with fungi and bacteria and the system is allowed to evaporate, dramatic changes are observed on the cells. AFM micrographs show disintegration of the hyphae of *Phomopsis phaseoli* and the cell walls of *Xanthomonas campestris* and *X. axonopodis*. Collapses to fungal and bacterial cells may be a result of

formation of pores triggered by micelles and lamellar structures, which are formed above the critical micellar concentration of lipopeptides. As observed for *P. phaseoli*, the process involves binding, solubilization, and formation of novel structures in which cell wall components are solubilized within lipopeptide vesicles. This is the first report presenting evidences that vesicles of uncharged and negatively charged lipopeptides can alter the morphology of gram-negative bacteria.

**Keywords** Antimicrobial peptides · Non-ribosomal peptides · Lipopeptides · Iturin · Surfactin · Atomic force microscope · *Bacillus subtilis* · *Xanthomonas*

### Abbreviations

AFM	Atomic force microscope
NRPS	Non-ribosomal peptide synthetase
OM	Optical microscopy
PKS	Polyketide synthase
PE	Plant emergence
PH	Plant height
PDW	Plant dry weight
Xac	<i>Xanthomonas axonopodis</i> pv. <i>citri</i>
Xcc	<i>Xanthomonas campestris</i> pv. <i>campestris</i>

Communicated by Jorge Membrillo-Hernández.

A. Etcheagaray (✉) · C. de Castro Bueno  
Faculdade de Química, PUC-Campinas,  
C. Postal 317, Campinas, SP 13012-970, Brazil  
e-mail: augusto.etcheagaray@puc-campinas.edu.br

I. S. de Melo  
Laboratório de Microbiologia,  
Embrapa Meio Ambiente, Jaguariuna, SP, Brazil

S. M. Tsai · M. de Fátima Fiore · M. E. Silva-Stenico  
CENA, Universidade de São Paulo,  
C. Postal 96, Piracicaba, SP 13400-970, Brazil

L. A. B. de Moraes  
Departamento de Química, Universidade de São Paulo,  
Av. Bandeirantes, Ribeirão Preto, SP 14100-000, Brazil

O. Teschke  
Laboratório de Nanoestruturas e Interfaces,  
Instituto de Física, UNICAMP,  
Campinas, SP 13083-970, Brazil

### Introduction

Several lipopeptides produced non-ribosomally have been identified in extracts of *Bacillus subtilis*. These can be grouped in three different classes; the surfactin, fengycin, and iturin families. Members of the surfactin and fengycin groups are composed of one  $\beta$ -hydroxy fatty acid and seven (surfactins) or ten (fengycins)  $\alpha$ -amino acids, while members of the iturin family contain a  $\beta$ -amino fatty acid linked

to seven  $\alpha$ -amino acids. The presence of the  $\beta$ -amino fatty acid is the most striking characteristic of the iturin A family and distinguishes this group from the other two (Maget-Dana and Peypoux 1994; Leclère et al. 2005). In all lipopeptide classes, the length of the fatty acid chain is variable, a minimal of 13 carbons is observed in surfactins, whereas in iturins the length starts with C<sub>14</sub> to a maximum of C<sub>17</sub>, and C<sub>18</sub> for fengycins. Thus homologous lipopeptides within each family can be found in *Bacillus* extracts (Razafindralambo et al. 1997).

Due to their size and amphipatic character, iturin A has a tendency to associate and form small vesicles (Grau et al. 2001), inducing the formation of pores in biological membranes (Aranda et al. 2005). In the specific interaction of iturins with phosphatidylcholine it was shown that these lipopeptides are arranged in small mixed-vesicles complexed with phosphatidylcholine molecules (Grau et al. 2001). Iturins also form aggregates with surfactins when both are present (Razafindralambo et al. 1997). The latter characteristic may also explain the synergistic effect of surfactin on the antifungal activity of iturins (Maget-Dana et al. 1992).

Iturins are interesting membrane-active antimicrobials, generally effective against fungal pathogens (Maget-Dana and Peypoux 1994; Romero et al. 2007). However, it has also been reported that iturins are effective against the phytopathogenic bacterium *Xanthomonas campestris* pv. *campestris* (Xcc) (Monteiro et al. 2005).

Microscopic examination of ultra-thin sections of yeast cells revealed that iturin A exerts its effect on the cytoplasmic membrane. Upon interaction with this lipopeptide, electrolytes, and other cytoplasmic components of yeast cells are released owing to an alteration of cell permeability and formation of pores (Thimon et al. 1995). However, no experiments have shown the results of a direct interaction of these non-ribosomal peptides with bacterial or fungal cells under the atomic force microscope (AFM). AFM provides three-dimensional images of the surface ultra-structure at molecular resolution. The technique requires minimal sample preparation and yet provides insights on the structure of microbial membranes (Dufrêne 2002). Most of the studies with AFM describe the interaction of positively charged peptides (mostly of ribosomal origin), which attach to the negatively charged cell wall of gram-negative bacteria and induce morphological modifications of the cells (da Silva and Teschke 2003; Meincken et al. 2005). The membrane of gram-negative bacteria, which is the target of most antimicrobial peptides, is not easily transposed by neutral and negatively charged peptides. A positive charge in the structure of the antibiotic is important for binding. The interaction of positively charged peptides with the negative surface of these cell walls is described by the carpet-binding and toroidal models (Meincken et al. 2005;

Allende et al. 2005). To our knowledge, the internalization of neutral peptides by gram-negative bacteria following similar models has not been described yet, except for siderophores, which bind to specific receptors (Sprencel et al. 2000).

In the present study, considering the soil environment where pathogenic microbes coexist with beneficial rhizobacteria, we selected to study the effect of lipopeptides produced by a plant-growth promoting rhizobacteria on fungal and bacterial pathogens. For this goal AFM topographic images were obtained, demonstrating dramatic morphological modifications induced by lipopeptide aggregates on Xcc cells. Production of antibiotics is also important for the growth promoting *Pseudomonas* spp. that induces suppression of the root disease of wheat (Cook et al. 1995). The results presented by AFM demonstrate the competence of iturin and surfactin-producing strains of *Bacillus* spp. to control fungal and bacterial pathogens.

## Materials and methods

### Strains and media

Strains of *Bacillus* spp. used in this work corresponding to field isolates collected from soybean and bean fungal pathogens were identified by morphological and biochemical methods (Ivanova et al. 1999). *Bacillus subtilis* (strain OG), was further characterized by genetic methods (described below). Fungal pathogens were obtained from the culture collection of the laboratory of microbiology, EMBRAPA Jaguariúna, SP, Brazil. Xcc and *Xanthomonas axonopodis* pv. *citri* (Xac), were a gift of Dr. Jesus A. Ferro (Universidade Estadual Paulista, UNESP, Jaboticabal, São Paulo, Brazil). *Bacillus* spp. was grown in Nutrient growth media (liquid and solid) at 28°C, whereas fungal strains were incubated in Potato Dextrose Agar (PDA). The *Xanthomonas* strains were inoculated from glycerol stocks on YCD agar plates (Kim et al. 2003) and were grown for 3 days at 28°C.

### Effect of rhizobacteria on plant growth

Soybean seeds from Embrapa seed collection were used. Measurements of plant emergence, plant height (PH), weights of aerial and root parts of the soybean plants were obtained. Experiments were organised in a completely randomised block design using one factor, 27 levels, four repetitions and six seeds for each repetition. Plant emergence (PE) experiments were designed in balanced randomised blocks, whereas the parameters of PH, aerial part- and root dry weight were designed using unbalanced completely randomised blocks. Seeds were superficially sterilised by treatment

with alcohol (70% ethanol, 3 min) and commercial sodium hypochlorite (5 min) followed by several washing steps in sterile water. After draining, they were imbedded in a suspension of rhizobacteria (approximately  $10^7$  CFU mL<sup>-1</sup>) and aseptically transferred to vases filled with non-sterile soil. Plant parameters were measured after 29 days of cultivation in the green house at temperatures ranging between 25 and 28°C. Measurements of PH were performed on the first day after harvest. Further determinations were obtained after rinsing the plants with water and drying at 105°C.

### Antimicrobial activity

#### *In vitro* assay

Dual culture assays were performed by co-cultivation experiments in PDA plates (Petri dishes). Plates were preliminarily inoculated with a disc (0.8 cm diameter) of *Phomopsis phaseoli* pv. *meridionalis*, which was removed from a 5-day-old culture grown at 28°C in PDA. The plug containing fungal mycelia was placed at 1.5 cm from one of the edges of the plate and incubated 24 h before the addition of the antagonist bacteria. Twenty micro liter of a cell suspension (approximately  $10^{10}$  cell mL<sup>-1</sup>) of the corresponding *Bacillus* strain was streaked at 1.5 cm of the opposite edge of the plate keeping a distance (4 cm) from the fungal inoculum. Paired cultures were incubated at 28°C for 3 days and inhibition was determined by measuring the distance between *P. phaseoli* and the corresponding *Bacillus* strain in comparison with a control without antagonist that was incubated along with the other Petri dishes.

#### Bioassay of lipopeptides

The inhibitory activity of iturins produced by selected *Bacilli* was evaluated by an agar diffusion method on PDA plates. Plates were inoculated with agar discs of the fungal strains on one side of the plate and with paper discs for addition of metabolites on the opposite side. Discs were placed at 1 cm from each of the edges of the plate and were diagonally separated by a distance of 8 cm. After solid-phase extraction (described below), lipopeptides were diluted to a concentration of 10 mg mL<sup>-1</sup> in 100% methanol. Five micro liter of lipopeptide solution was added directly on the filter discs. All operations were performed under sterile conditions. The inhibitory activity was estimated from measurements of fungal growth across the line separating the discs compared to a control in which only methanol was added.

#### Extraction of lipopeptides

Production of anti-fungal lipopeptides by novel isolates of *B. subtilis* was evaluated using previously described growth

conditions (Besson et al. 1976) and extraction procedure (Razafindralambo et al. 1993). Cells were grown in liquid media and metabolites were extracted from the supernatant on C-18 cartridges (Extract-clean Hi-Load 10 g C-18 cartridge, Altech Associates Inc., Deerfield, IL).

Culture supernatants were loaded onto cartridges and the hydrophobic material was eluted as described below. Columns were firstly washed with 50% methanol in water, followed by elution of lipopeptides with 100% methanol. After elution, extracts were concentrated under vacuum and analysed by high performance liquid chromatography (HPLC) using the Äkta Basic system (Amersham Pharmacia Biotech UK Limited, Buckinghamshire, England) equipped with a continuous absorption monitor in the range of 190–900 nm. Peaks were monitored in the wavelengths of 214, 254 and 280 nm. Chromatography followed conditions previously described (Razafindralambo et al. 1993). The HPLC column was pepRPC HR 5.5 (a C2-C18 reversed-phase column). An elution gradient was prepared with solvent A (0.1% TFA in water) and solvent B [0.1% TFA in water:acetonitrile (30:70)]. Gradient conditions were set: 0–45% B (20 mL); 45–60% B (11 mL); 60–80% B (11 mL); 80–100% B (0 mL); 100% B (5 mL). Under the above conditions, iturin A (generously given by Doctor Alan Lax, USDA, USA) was eluted at 25 min.

#### Determination of minimum inhibitory concentrations (MIC)

Cells of *Xac* and *Xcc* were incubated with diluted lipopeptide solutions as described. Bacterial cells were grown in liquid media to an absorbance (OD<sub>600 nm</sub>) of 0.6–0.8. Cells were collected by centrifugation and resuspended in Tris-HCl 20 mmol L<sup>-1</sup>, pH 8.0. These were adjusted to an OD<sub>600 nm</sub> of 0.4 in the presence of the following concentrations of lipopeptides dissolved in the same buffer and sterilized by filtration: (135 mg mL<sup>-1</sup>; 67.5 mg mL<sup>-1</sup>; 33.75 mg mL<sup>-1</sup> and 13.5 mg mL<sup>-1</sup>). After 60 min of incubation, cells were diluted and transferred to Petri dishes containing YCD media and incubated. Duplicate plates were prepared for each dilution. Analysis of colony forming units (cfu) was performed after 3 days of incubation at 28°C. The MIC was considered based on a reduction of cfu greater than 50%.

#### Mass spectrometry (MS) analysis

MS analyses were performed in a hybrid quadrupole time-of-flight (Q-TOF) mass spectrometer from Micromass (Manchester, UK) equipped with an electrospray ion source (ESI). Experiments were performed under high resolution and high accuracy (5 ppm). Conditions for positive ESI were as follows, the desolvation gas (N<sub>2</sub>) was heated at

150°C, the capillary was held at a potential of 3.5 kV, and the cone voltage was 25 V. The lipopeptide extract of *B. subtilis* was dissolved in a mixture of methanol and formic acid 1:1 (v/v) and analyzed in positive ion mode. Sample was introduced into the source at 5  $\mu\text{L min}^{-1}$  with a syringe pump.

#### Strain characterization by molecular biology

Cells from strain 0G were collected by centrifugation at 13,000g for 15 min at 4°C. The pellet was washed three times with sterilized ultrapure water (centrifuged at 13,000 $\times$ g for 15 min at 4°C) and stored at –20°C. After thawing the stored samples, the DNA was extracted using the FastDNA Kit (Q-Biogene, Carlsbad, CA, USA) according to the manufacturer's specifications. Integrity of the extracted DNA was verified by electrophoretic analysis using 1% agarose gel stained with ethidium bromide. Gels were viewed on a Fluor-S Multi-Imager (BioRad, Hercules, CA, USA) and recorded.

The 16S rRNA sequence was amplified from genomic DNA using the specific primer-set 27F1 and 1494R (Neilan et al. 1997). Amplification was performed in a 25  $\mu\text{L}$  polymerase chain reaction (PCR) containing 10 ng of genomic DNA, 5 pmol  $\mu\text{L}^{-1}$  of each oligonucleotide primer, 10 mM of each dNTP, 50 mM  $\text{MgCl}_2$ , 10 $\times$  PCR buffer and 5 U Platinum *Taq* DNA polymerase (Invitrogen, Carlsbad, CA, USA). A Gene Amp PCR System 2400 (Applied Biosystems, Foster City, CA, EUA) was used. Thermal cycling was performed with an initial denaturation step at 94°C for 4 min, followed by 30 cycles of DNA denaturation at 94°C for 20 s, primer annealing at 50°C for 30 s, strand extension at 72°C for 2 min, and a final extension step at 72°C for 7 min. PCR products were analyzed by electrophoresis. New PCR products were cloned using a pGem-T Easy kit (Promega, Madison, WI, USA) according to manufacturer's instructions. Competent *E. coli* DH5 $\alpha$  cells were used for transformations. Recombinant plasmids were isolated from specific clones according to standard procedures (Birnboim and Doly 1979). For DNA sequencing the DYE-namic ET Terminator Cycle Sequencing Kit from Amersham Biosciences (UK) was used. An external and three internal primer sets (Lane 1991) were used for the complete sequencing of the 16S rRNA. The cycle sequencing reaction included 25 cycles of 10 s at 95°C, 5 s at 50°C, and 4 min at 60°C. After the sequencing reaction was completed, samples were sequenced in an ABI PRISM 310 Genetic Analyzer (Applied Biosystems) following manufacturer's instructions.

The 16S rRNA sequences obtained in this study were aligned with related sequences retrieved from GenBank using the Clustal X program (Thompson et al. 1997). Phylogenetic trees were constructed by neighbour-joining (NJ) and maximum-parsimony (MP) algorithms using the

MEGA package version 3.1 (Kumar et al. 2004). The NJ and MP stability of the relationships was assessed by bootstrapping (1,000 replicates). Comparative sequence analysis by BLAST (Altschul et al. 1990) involved selection of the closest cultured strain when the best hit came from uncultured clones.

The 16s rRNA sequence was deposited in GenBank under accession number EF666489.

#### Atomic Force Microscope

Fungal and bacterial cells were either directly added to mica or previously incubated with lipopeptides. A loop full of bacterial cells or fungal mycelia was suspended in 1 mL of water before the addition of lipopeptides. Lipopeptides were incubated with cells at room temperature for 15 min, after which a drop of 10  $\mu\text{L}$  of the suspension was deposited on mica. Before analysis the latter sample was left to evaporate for 24 h under ~60% humidity.

The ThermoMicroscope AutoProbe CP was used for these experiments. A cantilever with ultra-low spring constants ( $\sim 0.03 \text{ N m}^{-1}$ , Park Scientific Instruments, Mountain View, CA, USA) allowed probing bacterial cells by contact mode without any physical damage. Before measurements, the size and shape of AFM probes were characterized using a reference sample of titanium. The imaging force was kept below 1 nN and the scan rate in the range of 1–4 Hz. The software TopoMetrix SPMLab, 4.0 was used to analyze AFM data. For additional morphological analyses the software SPM Image Magic (<http://www.geocities.com/SiliconValley/Network/6216/>) was used. Lipopeptides directly added to substrates (silicon and mica) were dehydrated as above and analyzed in the non-contact mode. Silicon wafers with a resistivity of 10  $\Omega \text{ cm}^{-1}$  (Virginia Semiconductor, Inc., VA, USA) were used. Fragments of approximately 1  $\times$  1  $\text{cm}^2$  were fixed in a 50% solution of HF for a few minutes and then rinsed with water. Muscovite mica from Mica New York Co (NY, USA) was used. Samples were deposited on freshly cleaved mica.

## Results

### Selection of competent strains of *Bacillus* spp

Strains were chosen based on their contribution for plant growth. The effects of rhizobacteria on the emergence of soybean were evaluated by growing the plants for 30 days in non-sterile soil. After treatment with 16 different isolates of *Bacillus* spp., the parameters of PE, PH and plant dry weight (PDW) were measured. PDW (including aerial and root parts) was used to compare the effects of *Bacillus* spp. with a control that received no treatment (Table 1). The

**Table 1** Parameters of soybean plants treated with *Bacillus* spp.

Isolate	Plant height <sup>a,b</sup> (cm)	Height gain <sup>c</sup> (%)	Plant dry weight <sup>a,b</sup> (mg)	Weight gain <sup>c</sup> (%)
Control	8.4 ± 0.9 (17)	–	178 ± 33 (17)	–
G2-6	9.9 ± 1.0 (13)	18 ± 1.9	193 ± 35 (13)	8 ± 0.9
G7-6	8.3 ± 0.8 (10)	–	196 ± 38 (10)	10 ± 1.2
G3-6C	9.0 ± 1.1 (11)	7 ± 0.8	184 ± 32 (11)	3 ± 0.3
G2-7	8.4 ± 1.1 (10)	–	174 ± 27 (10)	–
5G	9.0 ± 1.3 (15)	7 ± 0.9	180 ± 30 (15)	1 ± 0.1
G1-6	9.8 ± 1.6 (15)	17 ± 1.9	198 ± 40 (15)	11 ± 1.0
G4-6	8.8 ± 1.5 (15)	5 ± 0.5	178 ± 26 (15)	–
OG	10.6 ± 1.9 (9)	26 ± 2.8	198 ± 37 (10)	11 ± 1.2
G11-6	9.0 ± 1.6 (17)	7 ± 0.6	163 ± 25 (18)	–
G3-6B	9.1 ± 1.4 (11)	8 ± 0.9	187 ± 28 (11)	5 ± 0.6
G11-5A	10.7 ± 2.0 (14)	27 ± 3.0	208 ± 39 (14)	17 ± 1.9
G8-7	10.8 ± 1.7 (14)	29 ± 3.0	187 ± 30 (15)	5 ± 0.6
G6-7	8.9 ± 1.0 (13)	6 ± 0.7	193 ± 30 (13)	8 ± 0.9
G9-6	9.1 ± 1.3 (11)	8 ± 0.9	197 ± 35 (11)	11 ± 1.3
18-G	9.5 ± 1.4(12)	13 ± 1.4	142 ± 21 (12)	–
G10-5C	10.2 ± 1.6 (14)	21 ± 2.3	144 ± 22 (15)	–

Plants were inoculated in non-sterile soil after treatment with isolates of *Bacillus*. The results presented correspond to an average of six repetitions with the number of plants for each repetition indicated in parenthesis

<sup>a</sup> Unbalanced—totally random

<sup>b</sup> Values in parenthesis represent the number of evaluated plants

<sup>c</sup> Height and weight gains were calculated by subtracting the average measured parameters from those obtained for plants that received no treatment (control)

results demonstrate that most of the strains contribute for plant growth. Selected strains were chosen for antifungal activity tests based on higher values of weight gain, calculated from the corresponding PDW.

#### Characterization of best isolates

Antifungal activity in dual-culture assays demonstrated that ten isolates of *B. subtilis* were inhibitory to *P. phaseoli*, presenting average growth inhibitory activity in the order of 40%. *B. subtilis* (strain OG), was considered the best antagonist of this fungus, with an average inhibitory activity of 63%. Experiments were repeated at least three times and presented a standard deviation (sd) of the mean of approximately 10%.

After solid-phase extraction, the lipopeptide fraction of selected strains (OG, 18G and G2-6) was adjusted to 5 mg mL<sup>-1</sup> in methanol, demonstrating inhibitory activity against *Rhizoctonia solani* and *Sclerotinia sclerotiorum* in agar plates. Average inhibition on the growth of the latter fungi was in the order of 14% (sd ~10%). The analyzed strains (OG, 18G and G2-6) presented lipopeptides of the

iturin and surfactin types as determined by HPLC (Fig. 1). Approximately 100 µg of extracted lipopeptides was injected in each analysis. The presence of iturin A in the extracts was confirmed by comparison with a standard. Additional lipopeptides were identified, potentially surfactins that according to Razafindralambo et al. (1993) are eluted at the end of the gradient. Considering that the latter late-peaks may correspond to surfactin, the HPLC peaks were accordingly labelled iturin- and surfactin-like peptides (Fig. 1). Mass-spectrometry analysis confirmed the presence of two isoforms of iturin (iturin A and iturin D), corroborated by tandem mass-spectrometry of the respective molecular ions [M + H]<sup>+</sup> at *m/z* 1043 and *m/z* 1057 (both indicated in Fig. 1b), which gave a fragmentation pattern similar to previously obtained by Gong et al. (2006).

#### Strain characterization by molecular biology

According to the 16s rRNA sequence analysis (Fig. 2), strain OG was most closely related to other *B. subtilis* strains, presenting 99% of sequence identity with all of the sequences used in the current analysis, being thus classified *B. subtilis*. Additional evidences that characterize the strain are amplification of non-ribosomal peptide synthetase (NRPS)-polyketide synthase/fatty acid synthase (PKS/FAS) genes using a multiplex PCR reaction (Etchegaray et al. 2004a). Performing such DNA amplification we obtained a PCR fragment of ~2.5 kb (data not shown), which is the expected size for the hybrid NRPS-FAS module of the NRPS involved in the biosynthesis of iturins (Tsuge et al. 2001).

#### Auto-organization of lipopeptides

A drop (10 µL) of a highly concentrated lipopeptide solution (5 mg mL<sup>-1</sup>) was added to silicon and muscovite mica and the system was allowed to dry for at least 24 h before analysis by AFM. Micrographs are shown in Fig. 3, where one can see the formation of aggregates in both substrates. On mica, the diameters of putative micelles are in the range of 150–300 nm, which correspond to aggregates with an area within (0.1–0.2 µm<sup>2</sup>). Larger aggregates may correspond to vesicles or lamellar structures, while those with diameters of about 150 nm may constitute micelles. However, possibly due to dehydration, layers of lipopeptides are formed making the structure grow vertically with peaks in the range of 4–5 nm (Fig. 3b). When the sample is allowed to dry on the substratum different patterns are observed on mica and silicon. The polar surface of mica contributes for spreading (Fig. 3a–b), whereas the hydrophobic surface of silicon concentrates solute at the border of the drop contributing to formation of larger aggregates (Fig. 3d), when compared to the center of the drop (Fig. 3c).

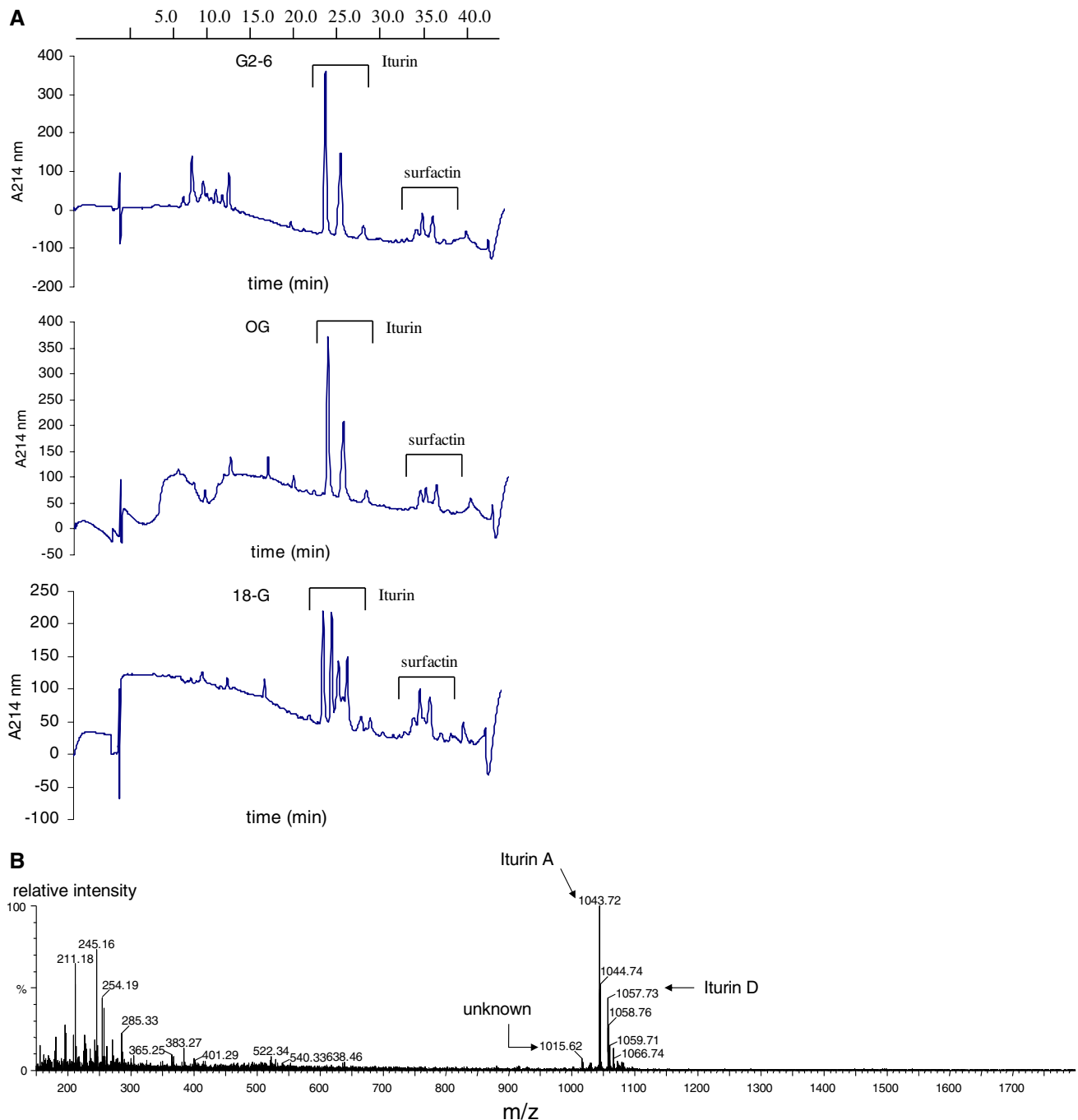


**Fig. 1** Analysis of the lipopeptide extract of *B. subtilis* (strains G2-6, OG and 18G) after solid-phase extraction. **a** HPLC chromatograms. **b** Q-TOF spectrum of the lipopeptide extract of strain OG, confirming the presence of iturin A, molecular ion  $[M + H]^+$   $m/z$  1043 Da; iturin

D, molecular ion  $[M + H]^+$   $m/z$  1057 Da. The peak labelled “unknown” may correspond to a surfactin isoform, molecular ion  $[M + Na]^+$  ( $m/z$ ) 1,015 Da

### Effect of lipopeptides on fungal mycelium

The soybean pathogen *Sclerotium rolfisii* was analyzed by optical microscopy (OM) and AFM before and after treatment with the isolated lipopeptides of strain OG. Iturin solutions with a concentration above the reported critical micellar concentration (CMC) of 20–80  $\mu\text{M}$  (Maget-Dana and Pey-

poux 1994) were used. Figure 4 shows the effect of lipopeptides on fungal hyphae. A reduction in hyphae structure is observed due to solubilization of cell wall by putative lipopeptide vesicles. Concomitantly, a novel structure is formed possibly composed by aggregates of lipopeptide and solubilized cell wall in addition to intracellular material. These mixed aggregates are formed with a 5 mM solution of

**Fig. 2** Phylogenetic characterization of isolate OG. The tree is based on the alignment of 16S rRNA sequences. Numbers near the nodes indicate bootstrap values over 50% for NJ and MP analyses. The sequence corresponding to *Bacillus subtilis* strain OG is highlighted

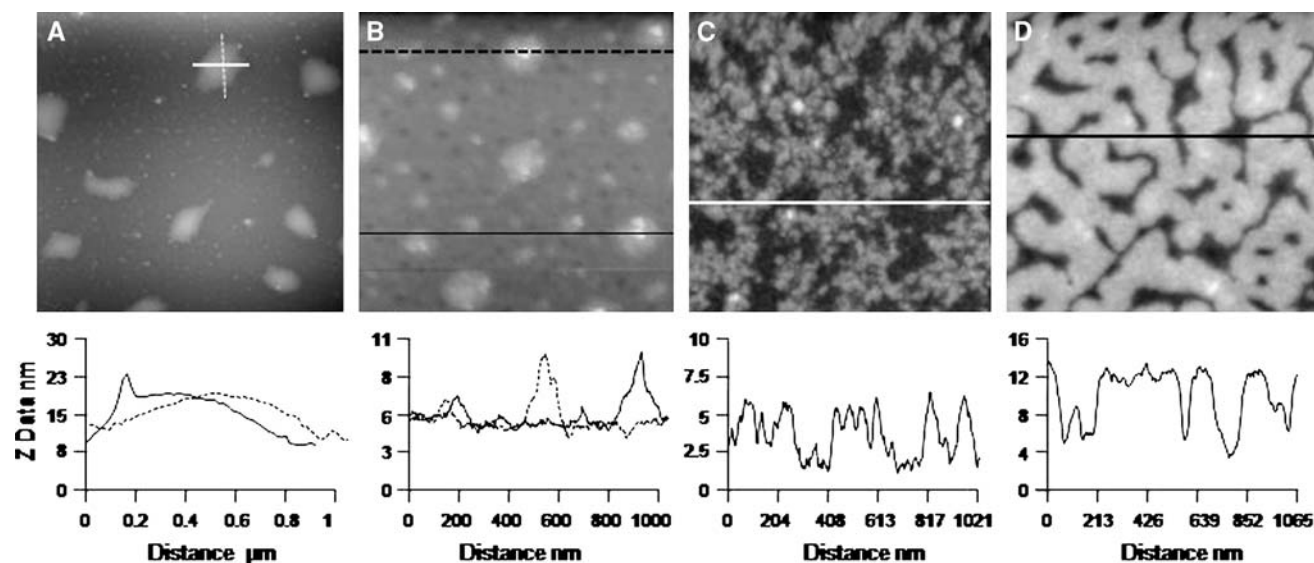
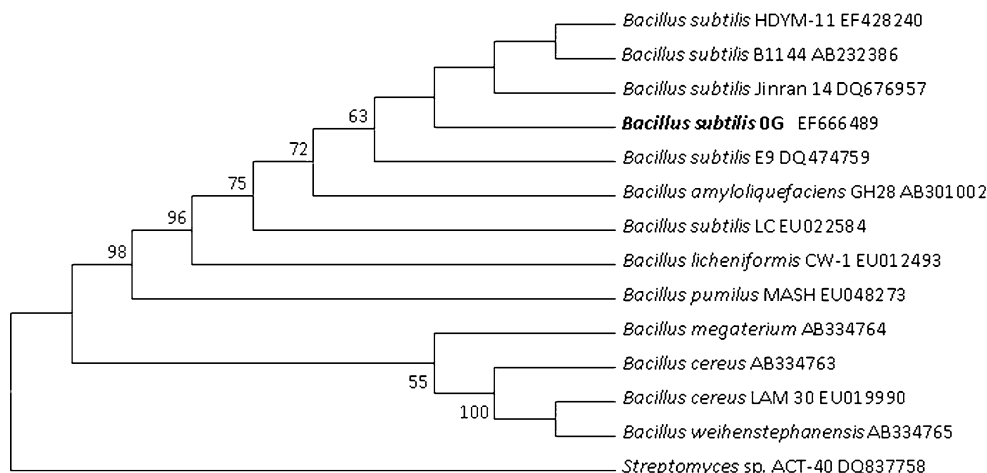


**Fig. 3** AFM micrographs of a dehydrated lipopeptide extract. Ten microliters of a lipopeptide solution (approximately  $5 \text{ mg mL}^{-1}$ ) was added to mica (a–b) and to silicon (c–d) and allowed to dry. The dimensions of selected aggregates are indicated in the corresponding

cross-sections below the micrograph. On mica (a–b), vesicles or lamellar structures are shown in a; micelles can be seen in b. Silicon micrographs also indicate formation of aggregates of various sizes, with very large structures formed at the border of the drop (d)

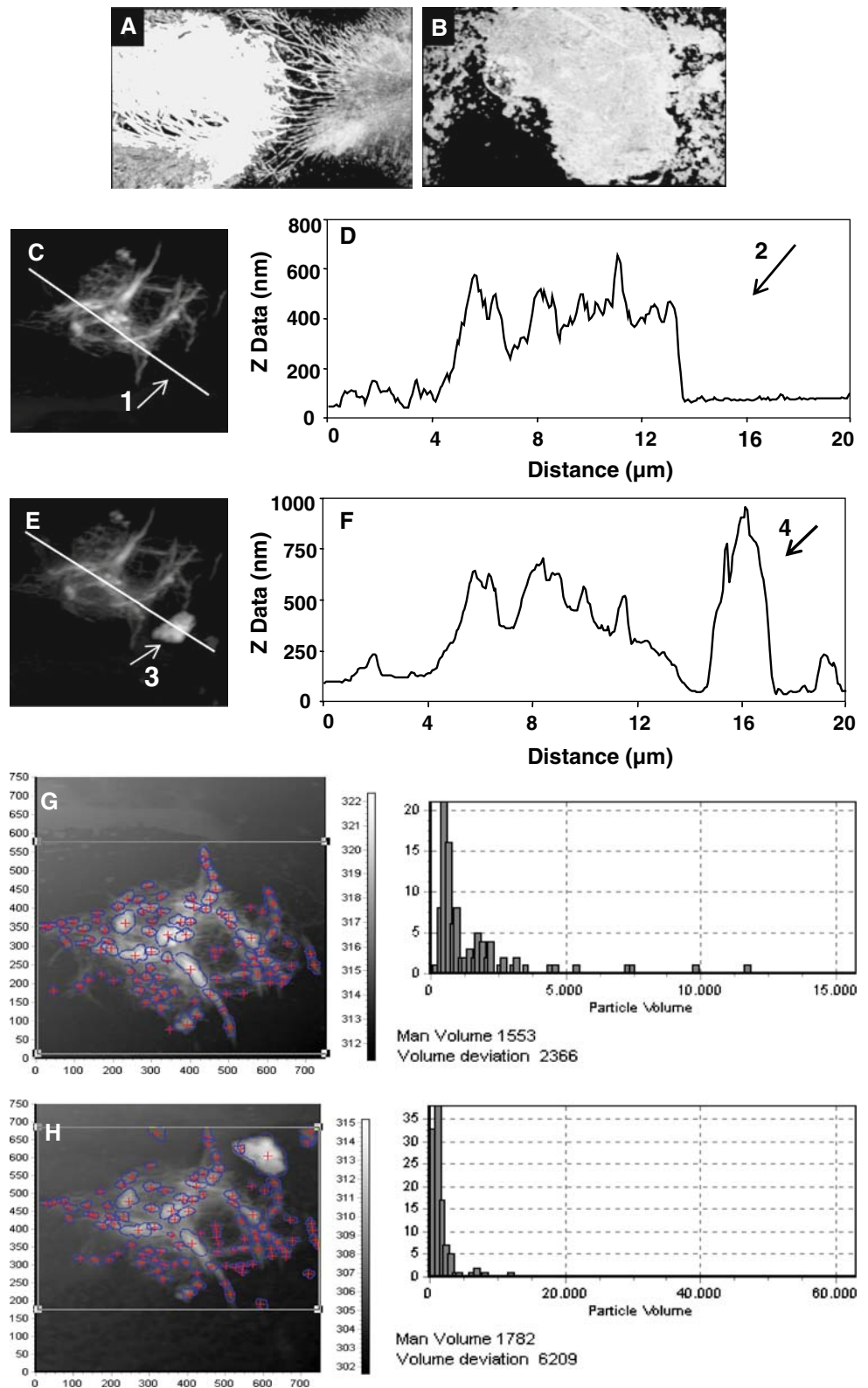
iturins (compare Fig. 4e–f). Although fungal cells were damaged by the lipopeptide treatment, an increase of 15% of volume of fungal/lipopeptide aggregates was observed. This is explained because the reduction in hyphae structure is compensated by formation of aggregates of lipopeptides and cell debris (indicated by arrows in Fig. 4). Complete disintegration occurs when cells are treated with a 100 mM solution of iturins as shown in the OM image of Fig. 4b, confirming a membrane solubilization effect.

#### Effect of lipopeptides on gram-negative bacterial cells

The plant pathogens Xcc and Xac were analyzed by AFM (Figs. 5, 6). Cells were treated with a high concentration of iturins (5 mM). An estimation of iturin concentration was obtained from HPLC analysis. Preliminary tests on the

effect of diluted solutions of lipopeptides on Xanthomonas cells indicated a MIC of  $68 \text{ mg mL}^{-1}$  for Xac (iturins approximately  $50 \text{ } \mu\text{mol L}^{-1}$ ) and  $14 \text{ mg mL}^{-1}$  (iturins approximately  $10 \text{ } \mu\text{mol L}^{-1}$ ) for Xcc. A very high concentration of lipopeptides induced dramatic changes on the morphology of Xcc cells, including shrinkage and leakage of intracellular material in addition to destruction of cell wall, possibly given by a solubilization effect. Before treatment with the lipopeptide solution (Fig. 5a), cells presented a layer possibly formed by extracellular polymeric substances (EPS) commonly associated with the virulence of Xanthomonas (Kamoun and Kado 1990). Considering the effect on Xcc cells, parameters by AFM before and after treatment with lipopeptides had average dimensions of  $2.4 \pm 0.3 \text{ } \mu\text{m}$  (length),  $1.6 \pm 0.2 \text{ } \mu\text{m}$  (width) and  $55 \pm 7 \text{ } \mu\text{m}$  (height). However, after treatment with antibi-

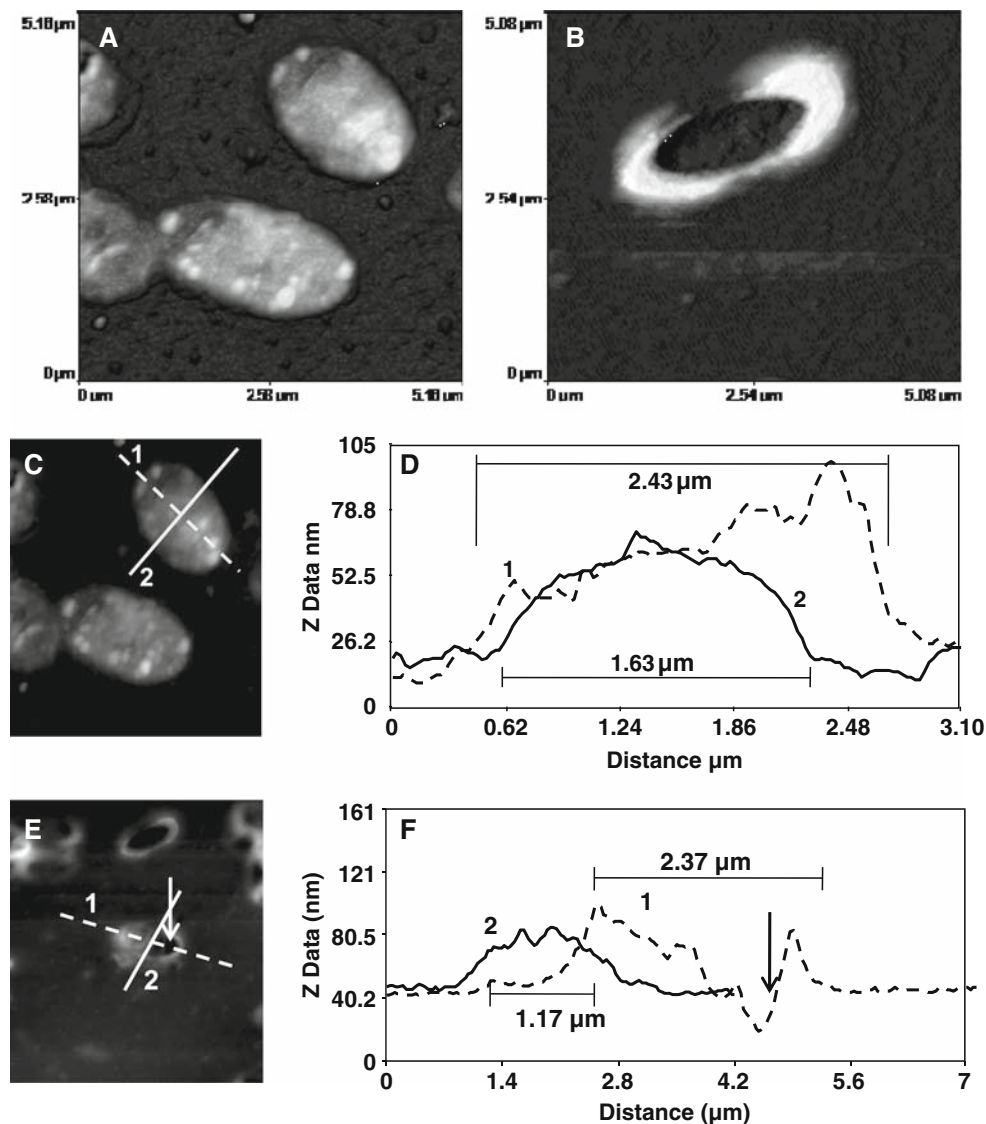
**Fig. 4** Effect of iturins on fungal cells. An optical microscopy (OM) micrograph with a magnification of 50 times is shown in **a** and **b**. Images corresponding to non-treated cells are shown in **a** (OM), **c** and **g** (AFM). Lipopeptide treated samples are shown in **b** (OM/100 mM iturins), **e** and **h** (AFM/5 mM iturins). In **d** and **f** the vertical profiles of cross-sections (*straight lines*) are shown. The AFM micrographs allow a comparison of the area indicated by the *arrows* before (1 and 2) and after (3 and 4) treatment with lipopeptides, demonstrating a reduction in fungal hyphae and formation of a novel structure. This is confirmed by the volumetric information before (**g**) and after (**h**) lipopeptide treatment, obtained using SPM Image Magic, which indicates an increment of 15% in volume



otic a dramatic decrease in cell height was observed within the boundaries of the cell. It is possible that EPS, cell debris, intracellular material, and lipopeptide mixed with hydrophobic constituents of the cell wall have accumulated at the

borders of the original cell structure (Fig. 5b–e). Fractal studies also confirm these observations. A fractal dimension greater than two is normally associated with volume (Christoforetti 1999; Ramakrishnan and Sadana 2002). Analysis

**Fig. 5** Effect of lipopeptides on Xcc cells observed by AFM. Images of Xcc were taken before treatment (a and c) and after treatment with lipopeptides (b and e). As shown, Xcc cells were completely disintegrated. Cell debris have accumulated at the borders of the original cell structure (b and e). Cross-sections of cells before and after lipopeptide treatment are shown in d and f. As indicated in both cases the hatched line (1) is associated with cell length, whereas the solid line (2) allows one to measure and observe the vertical profile associated to the width of the cell. An arrow in e and f indicates a major groove within the damaged cell



performed with the Gwyddion 2.5 software produced a fractal dimension of 2.30 for Xcc cells before the addition of lipopeptides. After treatment, a dimension of 1.68 was obtained, indicating that cells lost the volumetric information. The effect of lipopeptides on Xac (Fig. 6) was not as dramatic as described for Xcc. Cells became flatter and crumpled after treatment with lipopeptides (Fig. 6b, e, f). Comparing the width of a Xac cell before (1.5  $\mu\text{m}$ ) and after lipopeptide treatment (2.4  $\mu\text{m}$ ) a swelling effect is observed. Additionally, a different degree of roughness was observed upon treatment with lipopeptides, a cell surface that was initially soft became crumpled (compare Fig. 6a–b).

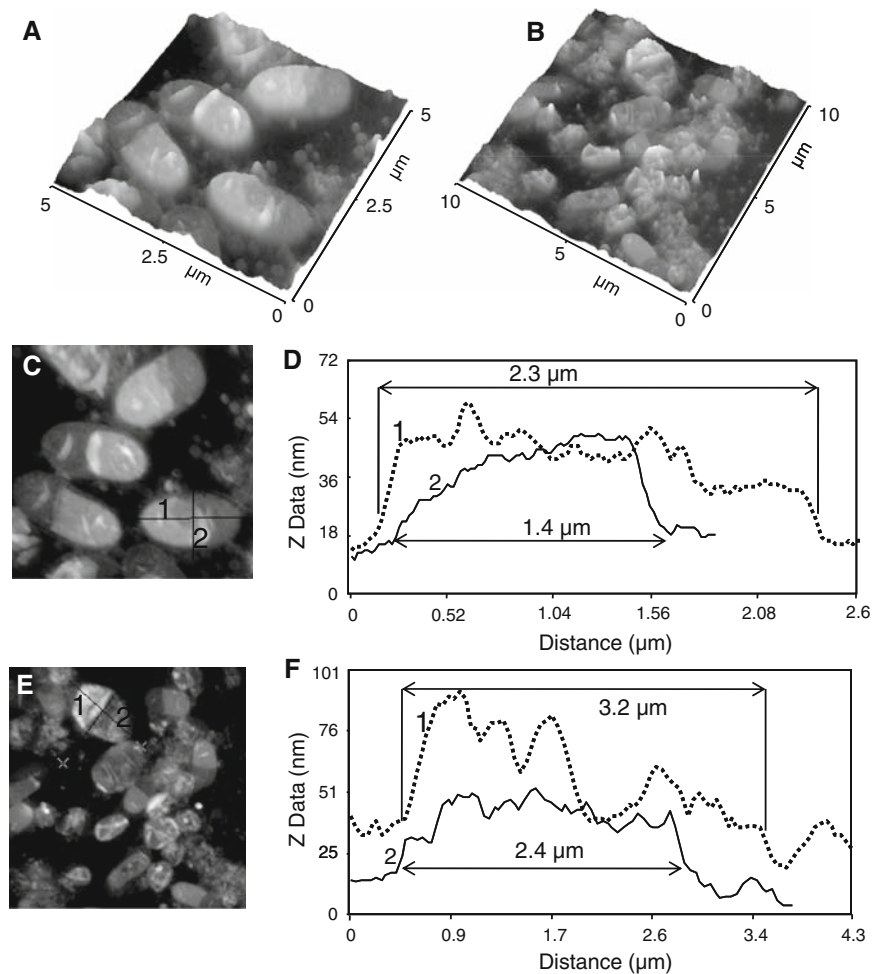
## Discussion

A great variety of chemical structures, including amino acid sequences that constitute peptide antibiotics, generates

positive, negative, and neutral antibiotics (Hancock and Chapple 1999). Contributing to structure diversity we find the non-ribosomally assembled peptides produced by bacteria and fungi (Etcheberry et al. 2004b).

Isoforms of the lipopeptides iturin and surfactin, two classes of non-ribosomal peptides produced by *B. subtilis* that have a cyclic peptide moiety linked to a fatty acid (Bonmatin et al. 2003), were found in the extract of *B. subtilis* strain OG. However, none of these are basic peptides, which are most active on bacterial membranes (Hancock and Chapple 1999). Iturins are neutral (Maget-Dana and Peypoux 1994) and surfactin is acidic, presenting a negative charge from mildly acid to high pH values (Maget-Dana and Ptak 1995). Two types of basic peptide antibiotics produced by *B. Subtilis* have been reported to date, the chlorotetaines (Phister et al. 2004) and the plipastatins (Umezawa et al. 1986; Tsuge et al. 1996). However, neither chlorotetaine ( $m/z$  289–291) nor plipastatin peaks ( $m/z$  in the range of

**Fig. 6** AFM micrographs showing the effect of lipopeptides on Xcc cells. Pictures **a** and **c** show images before the addition of lipopeptides. Micrographs **b** and **e** correspond to lipopeptide treated cells. Damages that can be observed are a swelling and crumpling effect (**b**). Cross-sections before (**d**) and after (**f**) lipopeptide treatment also contribute to these conclusions (cell dimensions are indicated)



1,460–1,500) were detected in the extract of strain OG (Fig. 1). Considering that the extraction procedure would remove the more polar chlorotetaines, we cannot ignore the possible contribution of plipastatins if present in lower amounts, since these were not detected by mass-spectrometry.

Iturins and surfactins form aggregates (micelles) at low concentrations and possibly lamellar structures at higher concentrations (Grau et al. 2001), which may enhance their membrane interaction capacity as observed in the case of amphotericin (Legrand et al. 1992). In our experiments, before imaging by AFM, samples were desiccated. Under dry conditions, the local concentration of lipopeptides is significantly increased, therefore auto-organization and formation of aggregates is induced. In fact AFM analysis of a concentrated solution of lipopeptides added to muscovite mica and silicon showed horizontal and vertical aggregation states (Fig. 3). Therefore, self-aggregation may be an important contribution for the membrane interaction and cell-morphology modifications induced by the lipopeptide extract on bacterial cells as previously observed by Legrand et al. (1992) for amphotericin.

The mode of action of positively charged anti-microbial peptides, which is based on a self-promoted uptake across

the cytoplasmic membrane, followed by interference with the cytoplasmic membrane barrier, is most commonly accepted (Hancock and Chapple 1999). The amphibian peptides magainins have been extensively studied. These ribosomally made peptides are known to form amphipatic alpha-helices, which are important for their mode of action against gram-negative bacteria (Oren and Shai 1998; Hancock and Chapple 1999). It is a rational that the cationic and hydrophobic nature of the molecule is important for the initial binding and internalization of the peptide antibiotic at the lipopolysaccharide layer of gram-negative bacteria. However, according to this model uncharged molecules such as iturins, would not bind to bacterial membranes or contribute to the formation of pores. Nevertheless, our results demonstrate that aggregates of iturins mixed with surfactin (also identified in the lipopeptide extract) due interact with gram-negative bacteria. AFM analysis demonstrates dramatic changes on cell morphologies induced by these lipopeptides.

When an area of 100 μm<sup>2</sup> of the mica surface containing bacterial cells was scanned and compared before and after incubation with lipopeptides, it was deduced that 100% of Xcc cells presented morphological modification including

dramatic volume reduction confirmed by fractal analysis. However, a similar analysis of the effect of lipopeptides on Xac cells indicated that approximately 36% of the cells within the 100  $\mu\text{m}^2$  area presented morphological modifications visualized by AFM. Fractal analysis of Xac cells did not show significant variations upon treatment (data not shown), one reason is that cells may have lost height but at the same time they became flat and swollen, thus keeping the same volume. In addition, lipopeptides attached to the cell surface may have contributed for the volume calculated by fractal analysis.

Whereas the antifungal activity of iturins and surfactins is well studied, the antibacterial action of iturins remains unsettled. The antibacterial activity of surfactins has been demonstrated at high concentrations (Vollenbroich et al. 1997; Huang et al. 2007). Another important application described for this lipopeptide is the binding at lipopolysaccharides in gram-negative bacteria with consequent reduction of septic shock (Hwang et al. 2007). Here, we have demonstrated that a mixture of iturins and surfactin at high concentration can bind and dramatically modify the surface of Xcc, a gram negative phytopathogen. A possible explanation for these results is that the mode of action of iturins may involve formation of mixed aggregates with other lipopeptides present in the extract including surfactin. These organized structures may remove positively charged cations such as calcium and/or magnesium that may be found attached to the negatively charged cell wall. Removal of cations can induce a collapse of the cell wall, contributing for lipopeptide integration into the membrane, and thus formation of pores. The chelating agent EDTA enhances the permeability of bacterial cells by a similar mechanism (Zhang et al. 2000; da Silva and Teschke 2003). In a study on the haemolytic activity of iturins it was found that these lipopeptides are able to induce leakage of intracellular compounds in human erythrocyte ghosts but not in large unilamellar liposomes, which are made of various kinds of lipids (Aranda et al. 2005). In analogy, the surface of Xac cells may not be as permeable as the surface of Xcc cells, possibly due to the presence of additional extracellular hydrophobic material. In a previous work we have identified a gene cluster in the genome of Xac, which might be involved in lipopeptide biosynthesis (Etcheagaray et al. 2004b).

In conclusion, considering that the lipopeptides present in the extract of strain OG have no positive charge, the present paper shows that an extract of iturin and surfactin was able to disintegrate the cell wall of the gram-negative phytopathogen Xcc. One possibility is that the affinity of iturins and surfactins for calcium may have promoted the uptake of these peptides into the negatively charged bacterial membrane by formation of positively-charged lipopeptide-calcium chelates. It has been shown by others that the

addition of calcium ions induce structural changes and penetration of surfactins on artificial phospholipid membranes (Knoblich et al. 1995). A potential source of calcium is the bacterial outer membrane (Nikaido 2003).

**Acknowledgments** This research has been funded by the Fundação de Pesquisa de São Paulo (Fapesp grants 96/11193-7 and 03/12529-4) and the Conselho Nacional de Pesquisa (CNPq). We would like to thank the valuable research assistance of L. O. Bonugli and J. R. Castro. M. E. Silva-Stenico was the recipient of postdoctoral fellowship from FAPESP (Grant 2004/16042-5)

## References

- Allende D, Simon SA, McIntosh TJ (2005) Melittin-induced bilayer leakage depends on lipid material properties: evidence for toroidal pores. *Biophys J* 88:1828–1837. doi:10.1529/biophysj.104.049817
- Altschul SF, Gish W, Miller W, Myers EW, Lipman DJ (1990) Basic local alignment search tool. *J Mol Biol* 215:403–410
- Aranda FJ, Teruel JA, Ortiz A (2005) Further aspects on the hemolytic activity of the antibiotic lipopeptide iturin A. *Biochim Biophys Acta* 1713:51–6. doi:10.1016/j.bbame.2005.05.003
- Birnboim HC, Doly J (1979) A rapid alkaline extraction procedure for screening recombinant plasmid DNA. *Nucleic Acids Res* 7:1513–1523
- Bonmatin J-M, Laprévotte O, Peypoux F (2003) Diversity among microbial cyclic lipopeptides: iturins and surfactins. Activity-structure relationships to design new bioactive agents. *Comb Chem High Throughput Screen* 6:541–556
- Besson F, Peypoux F, Michel G, Delcambe L (1976) Characterization of iturin A in antibiotics from various strains of *Bacillus subtilis*. *J Antibiot* 29:1043–1049
- Christofoletti A (1999) Modelagem de Sistemas Ambientais. Edgard Blucher, São Paulo
- Cook RJ, Thomashow LS, Weller DM, Fujimoto D, Mazzola M, Banger G, Kim DS (1995) Molecular mechanisms of defense by rhizobacteria against root disease. *Proc Natl Acad Sci USA* 92:4197–4201
- da Silva A Jr, Teschke O (2003) Effects of the antimicrobial peptide PGLa on live *Escherichia coli*. *Bioch Biophys Acta* 1643:95–103. doi:10.1016/j.bbamer.2003.10.001
- Dufrêne YF (2002) Atomic force microscopy, a powerful tool in microbiology. *J Bacteriol* 184:5205–5213. doi:10.1128/JB.184.19.5205-5213.2002
- Etcheagaray A, Rabello E, Dieckmann R, Moon DH, Fiore MF, von Döhren H, Tsai SM, Neilan BA (2004a) Algicide production by the filamentous cyanobacterium *Fischerella* sp. CENA 19. *J Appl Phycol* 16:237–243. doi:10.1023/B:JAPH.0000048509.77816.5e
- Etcheagaray A, Silva-Stenico ME, Moon DH, Tsai SM (2004b) *In silico* analysis of nonribosomal peptide synthetases of *Xanthomonas axonopodis* pv. citri: identification of putative siderophore and lipopeptide biosynthetic genes. *Microbiol Res* 159:425–437. doi:10.1016/j.micres.2004.09.009
- Gong M, Wang JD, Zhang J, Yang H, Lu XF, Pei Y, Cheng JQ (2006) Study of the antifungal ability of *Bacillus subtilis* strain PY-1 in vitro and identification of its antifungal substance (iturin A). *Acta Biochim Biophys Sin* 38:233–240. doi:10.1111/j.1745-7270.2006.00157.x
- Grau A, Gómez-Fernández JC, Peypoux F, Ortiz A (2001) Aggregational behavior of aqueous dispersions of the antifungal lipopeptide iturin A. *Peptides* 22:1–5. doi:10.1016/S0196-9781(00)00350-8

- Hancock RE, Chapple DS (1999) Peptide antibiotics. *Antimicrob Agents Chemother* 43:1317–1323
- Huang X, Wei Z, Zhao G, Gao X, Yang S, Cui Y (2007) Optimization of sterilization of *Escherichia coli* in milk by surfactin and fengycin using a response surface method. *Curr Microbiol* 56:376–381. doi:10.1007/s00284-007-9066-8
- Hwang YH, Park BK, Lim JH, Kim MS, Park SC, Hwang MH, Yun HI (2007) Lipopolysaccharide-binding and neutralizing activities of surfactin C in experimental models of septic shock. *Eur J Pharmacol* 556:166–171. doi:10.1016/j.ejphar.2006.10.031
- Ivanova EP, Vysotskii MV, Svetashev VI, Nedashkovskaya OI, Gorskhkova NM, Mikhailov VV, Yumoto N, Shigeri Y, Taguchi T, Yoshikawa S (1999) Characterization of *Bacillus* strains of marine origin. *Int Microbiol* 2:267–271
- Kim JG, Park BK, Yoo CH, Jeon E, Oh J, Hwang I (2003) Characterization of the *Xanthomonas axonopodis* pv. *glycines* Hrp pathogenicity island. *J Bacteriol* 185:3155–3166. doi:10.1128/JB.185.10.3155-3166.2003
- Knoblich A, Matsumoto M, Ishiguro R, Murata K, Fujiyoshi Y, Ishigami Y, Osman M (1995) Electron cryo-microscopic studies on micellar shape and size of surfactin, an anionic lipopeptide. *Coll Surf Biointerf* 5:43–48. doi:10.1016/0927-7765(95)01207-Y
- Kumar S, Tamura K, Nei M (2004) MEGA3: integrated software for molecular evolutionary genetics analysis and sequence alignment. *Brief Bioinform* 5:150–163
- Lane DJ (1991) 16S/23S rRNA sequencing. In: Stackebrandt E, Goodfellow M (eds) *Nucleic acid techniques in bacterial systematics*. Chichester, Wiley, pp 115–175
- Legrand P, Romero EA, Cohen BE, Bolard J (1992) Effects of aggregation and solvent on the toxicity of amphotericin B to human erythrocytes. *Antimicrob Agents Chemother* 36:2518–2522
- Leclère V, Béchet M, Adam A, Guez JS, Wathélet B, Ongena M, Thonart P, Gancel F, Chollet-Imbert M, Jacques P (2005) Mycosubtilin overproduction by *Bacillus subtilis* BBG100 enhances the organism's antagonistic and biocontrol activities. *Appl Environ Microbiol* 71:4577–4584
- Maget-Dana R, Peypoux F (1994) Iturins, a special class of pore-forming lipopeptides: biological and physicochemical properties. *Toxicol* 8:151–74
- Maget-Dana R, Ptak M (1995) Interactions of surfactin with membrane models. *Biophys J* 68:1937–1943
- Maget-Dana R, Thimon L, Peypoux F, Ptak M (1992) Surfactin/iturin A interactions may explain the synergistic effect of surfactin on the biological properties of iturin A. *Biochimie* 74:1047–1051
- Monteiro L, Mariano RLR, Souto-Maior AM (2005) Antagonism of *Bacillus* spp. against *Xanthomonas campestris*. *Braz Arch Biol Technol* 48:23–29
- Meincken M, Holroyd DL, Rautenbach M (2005) Atomic force microscopy study of the effect of antimicrobial peptides on the cell envelope of *Escherichia coli*. *Antimicrob agents chemother* 49:4085–4092. doi:10.1128/AAC.49.10.4085-4092.2005
- Neilan BA, Jacobs D, Del Dot T, Blackall LL, Hawkins PR, Cox PT, Goodman AE (1997) rRNA sequences and evolutionary relationships among toxic and nontoxic cyanobacteria of the genus *Microcystis*. *Int J Syst Bacteriol* 47:693–697
- Nikaido H (2003) Molecular Basis of bacterial outer membrane permeability revisited. *Microbiol Mol Biol Rev* 67:593–656. doi:10.1128/MMBR.67.4.593-656.2003
- Oren Z, Shai Y (1998) Mode of action of linear amphipathic alpha-helical peptides. *Biopolymers* 47:451–463
- Phister TG, O'Sullivan DJ, McKay LL (2004) Identification of bacillisin, chlorotetaine, and iturin A produced by *Bacillus* sp. strain CS93 isolated from pozol, a Mexican fermented maize dough. *Appl Environ Microbiol* 70:631–634. doi:10.1128/AEM.70.1.631-634.2004
- Ramakrishnan A, Sadana A (2002) A mathematical analysis using fractals for binding interactions of nuclear estrogen receptors occurring on biosensor surfaces. *Anal Biochem* 303:78–92. doi:10.1006/abio.2002.5581
- Razafindralambo H, Popineau Y, Deleu M, Hbid C, Jacques P, Tonart P, Paquot M (1997) Surface-active properties of surfactin/iturin A mixtures produced by *Bacillus subtilis*. *Langmuir* 13:6026–6031
- Razafindralambo H, Paquot M, Hbid C, Jacques P, Destain J, Thonart P (1993) Purification of antifungal lipopeptides by reversed-phase high-performance liquid chromatography. *J Chromatogr* 639:81–85
- Romero D, de Vicente A, Olmos JL, Dávila JC, Pérez-García A (2007) Effect of lipopeptides of antagonistic strains of *Bacillus subtilis* on the morphology and ultrastructure of the cucurbit fungal pathogen *Podosphaera fusca*. *Appl Microbiol* 103:969–976. doi:10.1111/j.1365-2672.2007.03433.x
- Sprencel C, Cao Z, Qi Z, Scott D, Montague M, Ivanoff N, Xu J, Raymond K, Newton S, Klebba P (2000) Binding of ferric enterobactin by the *Escherichia coli* periplasmic protein FepB. *J Bacteriol* 182:5359–5364
- Thimon L, Peypoux F, Wallach J, Michel G (1995) Effect of the lipopeptide antibiotic, iturin A, on morphology and membrane ultrastructure of yeast cells. *FEMS Microbiol Lett* 128:101–106
- Thompson JD, Gibson TJ, Plewniak F, Jeanmougin F, Higgins DG (1997) The CLUSTAL\_X windows interface: flexible strategies for multiple sequence alignment aided by quality analysis tools. *Nucleic Acids Res* 25:4876–4882
- Tsuge K, Akiyama T, Shoda M (2001) Cloning, Sequencing, and Characterization of the Iturin A Operon. *J Bacteriol* 183:6265–6273
- Tsuge K, Ano T, Shoda M (1996) Isolation of a gene essential for biosynthesis of the lipopeptide antibiotics plipastatin B1 and surfactin in *Bacillus subtilis* YB8. *Arch Microbiol* 165:243–251
- Umezawa H, Aoyagi T, Nishikiori T, Okuyama A, Yamagishi Y, Hamada M, Takeuchi T (1986) Plipastatins: new inhibitors of phospholipase A2, produced by *Bacillus cereus* BMG302-fF67. I. Taxonomy, production, isolation and preliminary characterization. *J Antibiot* 39:737–44
- Vollenbroich D, Pauli G, Muhsin OZ, Vater J (1997) Antimycoplasmal properties and application in cell culture of surfactin, a lipopeptide antibiotic from *Bacillus subtilis*. *Appl Environ Microbiol* 63:44–49
- Zhang L, Dhillon P, Yan H, Farmer S, Hancock REW (2000) Interactions of bacterial cationic peptide antibiotics with outer and cytoplasmic membranes of *Pseudomonas aeruginosa*. *Antimicrob agents chemother* 44:3317–3321